IRSTI 55.23.09 https://doi.org/10.26577/phst.2023.v10.i2.04

Synthesis of hierarchical WO_3 microspheres for photoelectrochemical water splitting application

A.A. Markhabayeva[1,*], R. Dupre[2], R. Nemkayeva[3] and N. Nuraje[4,5*]

[1] Institute of Applied Science and Information Technologies, Almaty, Kazakhstan
[2] Department of Chemical Engineering, Texas Tech University, Lubbock, Texas, United States
[3] Department of Chemical and Materials Engineering, School of Engineering and Digital Science, Nazarbayev University, Astana, Kazakhstan
[4] Renewable Energy Lab, National Laboratory Astana, Nazarbayev University, Astana, Kazakhstan
*e-mail: aiko.marx87@gmail.com, nurxat.nuraje@nu.edu.kz

(Received September 12, 2023; received in revised form October 10, 2023; accepted November 4, 2023)

In this work, hierarchical WO_3 microspheres were synthesized using chemical bath deposition. The morphology of the synthesized sample was studied using scanning electron microscopy (SEM). The hierarchical WO_3 microspheres formed from spontaneously self-assembled nanosheets have a high specific surface area. Structural characterizations of sample were performed using X-ray diffraction (XRD) and Raman spectroscopy. Analysis of XRD spectra showed that synthesized particles have a monoclinic modification. The optical properties of the sample were studied using UV-Vis diffuse reflectance absorption spectra. The value of the energy gap calculated from the absorption spectra is 2.25 eV, which indicates high light absorption ability. A photocurrent study was done to investigate the photocatalytic activity. The photoelectrode was prepared using hierarchical WO_3 microspheres and polymer deposited on fluorine doped tin oxide (FTO) glass via spin coating technique. A remarkable photocurrent density of 18 $\mu A/cm^2$ at 0.5 V was achieved. The elongated structures improved light absorption ability and photocatalytic activity, and might be perspective as photoanode in photoelectrochemical cells.

Key words: nanoparticles, tungsten oxide, photocatalysts, water splitting, microspheres.
PACS numbers: 88.40.-j, 78.20.-e.

1 Introduction

In recent years, the conversion of solar radiation into practical forms of energy remains a scientific and engineering challenge in the context of fulfilling human energy demands. Photocatalytic water splitting is a technology that utilizes solar energy to drive a chemical reaction that splits water (H_2O) into its constituent elements: hydrogen (H_2) and oxygen (O_2). This process involves the use of a photocatalyst, a material that can absorb light energy and facilitate the necessary reactions. The absorbed photons provide enough energy to excite electrons in the photocatalyst to higher energy levels, leaving behind positively charged "holes" in their original positions. The excited electrons and holes participate in separate reactions. The electrons are involved in the reduction of water ($4H^+ + 4e^- \rightarrow 2H_2$) to form hydrogen gas. The holes participate in the oxidation of water molecules, producing oxygen gas ($2H_2O \rightarrow O_2 + 4H^+ + 4e^-$). Therefore, the positions of the valence band (VB) and conduction band (CB) in a semiconductor material are main issue in terms of their energy levels relative to a reference electrode [1-4]. Tungsten oxide (WO_3) and its nanocomposites are actively used as photoactive nanomaterials in applications involving photoelectrochemical cells (PECs) [5-7]. This is due to their outstanding characteristics including photostability, a high electron mobility of approximately ~12 $cm^2 V^{-1} s^{-1}$, and extensive hole-diffusion length of about ~150 nm, the ability to absorb around of ~12% visible light, and cost-effectiveness [8]. WO_3 has a CB energy of +0.4 V relative to the NHE (normal hydrogen electrode) potential at pH = 0, while the valence band maximum is located at +3.1 V relative to the NHE potential, which is energetically favorable for water oxidation.

According to some works results, it was demonstrated, that rational synthesis of semiconductor materials could provide active sides for catalysts [9-

12]. Recently, flower like g-C_3N_4/NiO photocatalyst demonstrated much higher activity for the removal of tetracycline and Cr^{6+} than traditional layered sample [13]. Zhang and other authors obtained B-doped $Bi_2O_2CO_3$ hierarchical microspheres with enhanced photocatalytic performance for NO removal [14]. Structure and morphology evolution mechanisms of hierarchical flower-like Nb_2O_5 microspheres have been suggested, and exhibits higher photocatalytic activity for photodegradation of Rhodamine B than commercial [15].

In this work, we report synthesis of spherical microparticles with high specific surface area through chemical bath deposition at 90^0C, and via calcination at 400^oC. Chemical bath deposition (CBD) is one of the simplest and low cost method for synthesis semiconductor films and powders. In our previous work, WO_3 nanoplates have achieved by CBD at a relatively low temperature~ 90 °C using citric acid and hydrochloric acid [4]. In this work, we kept the low temperature ~ 90 °C, at normal atmospheric pressure due to simplicity.

In many studies, the effect of inorganic compound to the functional properties of synthesized nanomaterials were established [16-19]. Ma and fellow researchers employed the topochemical method with Na_2WO_4 and tetrafluoroboric acid HBF_4 to produce tungsten oxide nanoplates for gas sensing applications. [20]. Meng and colleagues [31] synthesized a flower-like hierarchical structure using citric acid $C_6H_8O_7$ and identified (-COOH) functional groups as key contributors to nanoplate growth [21-23]. In this work, we replaced the inorganic compound to the nitric acid and studied characteristics such as optical absorption and photoelectrochemical activity. It was found, that using nitric acid leads to the formation of WO_3 microparticles, which have good photoresponse.

2 Materials and methods

2.1 Chemicals and materials

Sodium tungstate dihydrate (Sigma Aldrich, purity >99%) and nitric acid (Acros Organics, purity 98%) were served as initial materials for the synthesis.

2.2 Procedure for synthesis of WO_3 particles

All chemicals were utilized as received without requiring further purification. WO_3 powders were generated through a chemical bath deposition method. To synthesize tungsten oxide nanopowders hydrothermally, an aqueous solution containing 0.1M sodium tungstate $Na_2WO_4 \cdot 2H_2O$ and 0.1M nitric acid was prepared. This solution was stirred at room temperature for 15 minutes and then placed in an oil bath set at approximately 90°C for 1 hour. Afterward, the resultant solution was allowed to cool to room temperature, followed by multiple washes with ethanol and water. The resulting samples were dried at 90°C under vacuum conditions for about 12 hours. Subsequently, a further thermal annealing process was conducted in a muffle furnace (SNOL 8.2/1100) at 400°C to achieve a polycrystalline phase of tungsten oxide nanopowders

2.3 Analysis and Techniques

The crystal phase composition and crystallinity of the products prepared were assessed using X-ray diffractometers: Rigaku Ultima III and MiniFlex Rigaku. X-ray diffraction patterns were acquired by scanning within the 2θ range of 5–90 °, with a step size of 0.02 ° and a scan rate of 0.33 min/degree. The X-ray source utilized was an X-ray tube with a copper anode, emitting CuKα radiation at a wavelength of 1.5418 Å, operating at a voltage of 40 kV and a current of 44 mA.

Raman spectra were recorded using the NTegra Spectra (NT-MDT) instrument with a blue laser having a wavelength of 473 nm. The exposure time was set at 30 s, and the laser spot diameter on the sample was approximately 2 μm. The laser power was maintained at 2 mW under 100% intensity. Scanning electron microscopy (SEM) images displayed in this study were captured using a Hitachi S4300 E/N FE-SEM field emission scanning electron microscope. Diffuse reflectance spectra of the samples were obtained using a Cary 5000 UV-Vis-NIR spectrophotometer equipped with an integrating sphere.

2.4 Measurements of photoelectrochemical characteristics

Photocurrent measurements were carried out using a Xenon solar lamp (AM 1.5G, 100mW/cm^2) with a UV-light filter, potentiostat (Corrtest CS310), and a quartz cell. All experiments pertaining to photoelectrochemical analysis were conducted at room temperature, employing a conventional three-electrode configuration with a platinum counter electrode and an Ag/AgCl reference electrode.The area of the working photoelectrode was 1.5 cm^2. An aqueous solution of electrolyte containing of H_2SO_4 (0.5 M) was used as an electrolyte. The Nernst equation is used to convert potentials: V_RHE=V_(Ag/AgCl)+0.0591 ×pH+ V_(Ag/AgCl)^0, where VAg/AgCl is the applied potential, V0Ag/AgCl is the standard potential of the Ag/AgCl reference electrode and pH is basicity or acidity of the electrolyte.

Briefly, 1 g of WO_3 particles and 0.05 g of polyvinylpyrolidone (PVP) were added to a 10 mL ethanol. Then, the slurry was stirred for 12 h to make a uniform suspension, followed by heating at 30 °C. The suspension was then deposited onto a cleaned FTO glass by a spin coating techique. A guided frame of 1 × 1.5 cm^2 area was built on the FTO glass using a tape to control the thickness and the coated area. Next, coated electrodes were heated at 320 °C for 60 min.

3 Results and discussion

Figure 1 illustrates scanning electron microscopy (SEM) visuals of the tungsten oxide nanopowders that were synthesized. The images exhibit spherical microparticles characterized by a rough surface. It's evident from the imagery that the microparticles have surfaces constructed from self-assembled nanosheets. The WO_3 particle sizes varied within the range of 1 µm to 3 µm, as depicted in Figure 1b.

In our case, the formation of 3D hierarchical WO_3 microspheres involves interaction of nanosheets during synthesis. As nanosheets continue to form, some of them might start to agglomerate, which means they clump together due to weak attractions between individual nanosheets. Over time, these agglomerates can undergo coalescence, where neighboring nanosheets merge into larger structures. During the coalescence process, smaller agglomerates with higher surface energy tend to dissolve and deposit material onto larger agglomerates with lower surface energy.

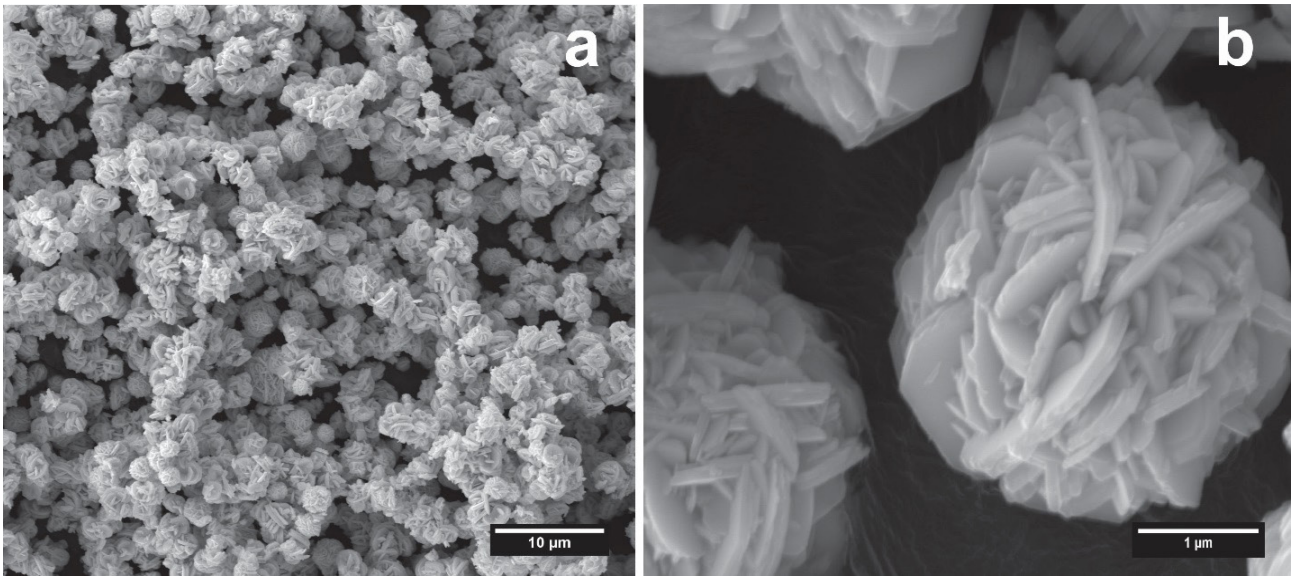

Figure 1 – SEM image of synthesized WO_3 microparticles

In Figure 2, the X-ray diffraction patterns of the WO_3 microparticles are depicted. The structure, aligning with the XRD data specified in the JCPDS No-01-083-0950 standard for the monoclinic form of tungsten trioxide.

Figure 3 presents the Raman spectra of WO_3 particles. The primary vibrational modes of tungsten oxide manifest within the frequency range of approximately ~ 805, ~ 710, ~ 270 cm^{-1}, corresponding to the stretching of the O-W-O bond, W-O bond, and the O-W-O bending, respectively (Daniel et al., 1987). [24]. Additionally, a group of weak peaks below 200 cm^{-1} is observed, attributed to lattice vibrations. Notably, sharp peaks around 270 and 324 cm^{-1} are associated with bending strain δ (O-W-O) [25].

The optical absorption characteristic of photocatalysts is important parameters. Since the obtained nanopowders are not transparent, the optical features of the samples were studied using UV-Vis diffuse reflectance spectra (UV-VIS Diffuse reflectance). The sample demonstrates absorption from UV to visible range of 500 nm, which makes it photocatalyst active in visible range and promising as photoanode material.

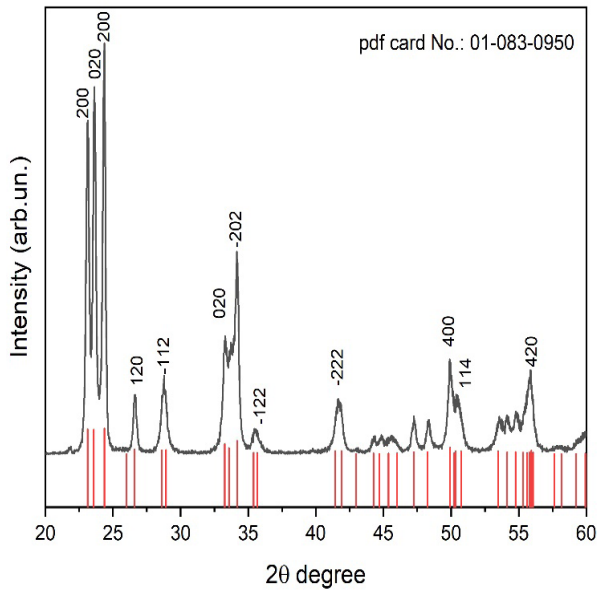

Figure 2 – XRD of the synthesized WO_3 microparticles

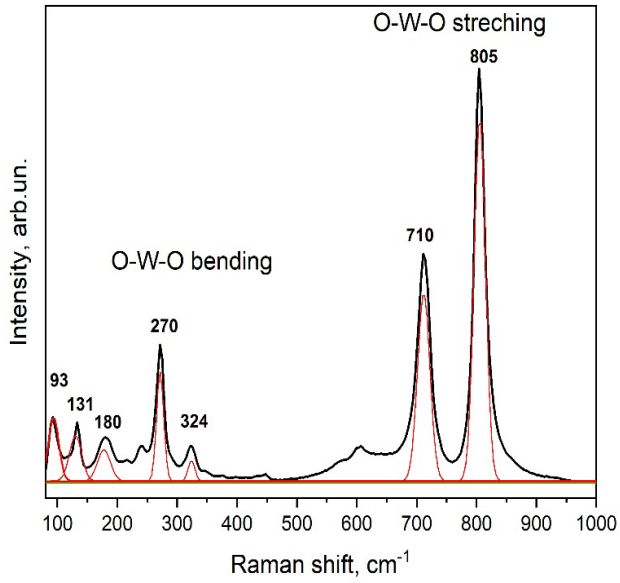

Figure 3 – Raman spectra of the synthesized WO_3 microparticles

In the upper right corner of Figure 4, the Tauc curve is shown, from which the optical bandgap of WO_3 particles was estimated using the equation:

$$\alpha h\nu = A(h\nu - E_g)^n \quad (1)$$

where:

α – the absorption coefficient;

E_g – is the optical bandgap of the semiconductor.

For crystalline semiconductors, n can take values of 1/2, 3/2, 2 or 3 when the transitions are direct allowed, direct forbidden, indirect allowed and indirect forbidden transitions, respectively. The bandgap of the obtained particles was estimated from the dependence of $(\alpha h\nu)^{1/2}$ versus $h\nu$. An extrapolation of the linear region of the curve to photon energy axis gives the value of band gap. Thus, for the synthesized material, bandgap energy is 2.25 eV, which indicates high light absorption ability [26, 27]. In the literature, the band gap of tungsten oxide is varying from 2.6 to 3 eV [28-30]. The redshift of optical absorption might be related with distinctive surface of the synthesized samples [31, 32].

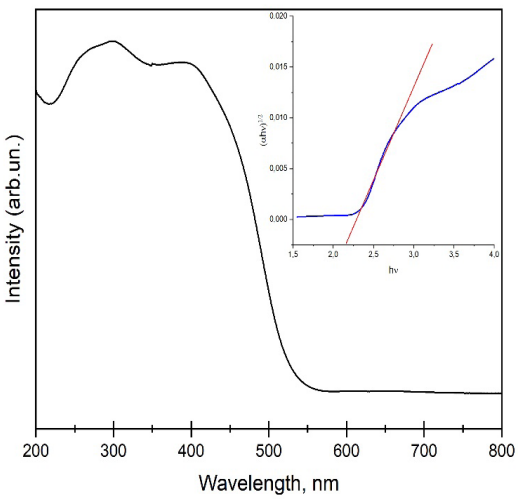

Figure 4 – UV-Vis diffuse reflectance absorption spectra of synthesized WO_3 particles. Plots of $(\alpha h\nu)^{1/2}$ vs. $h\nu$ (insert)

The photocatalytic performance of the WO_3 photoelectrode was evaluated by the photocurrent response under simulated sunlight irradiation. The chronoamperometry experiment at 0.5 V vs. Ag/AgCl was conducted under chopped illumination by swithcing simulated light on or off with each time duration of 10 sec as illustrated in Figure 5a. As expected, negligible current in the dark condition is observed. Under illumination, the significant current value of 18 μA/cm^2 appears. Linear sweep voltammetry (LSV) under chopped simulated solar light conditions was recorded at scan rate of 10mV/sec from 0 to 2V potential ranges. The results of chronoamperometry is in good agreement with the LSV results. The photocurrent increases with increasing voltage.

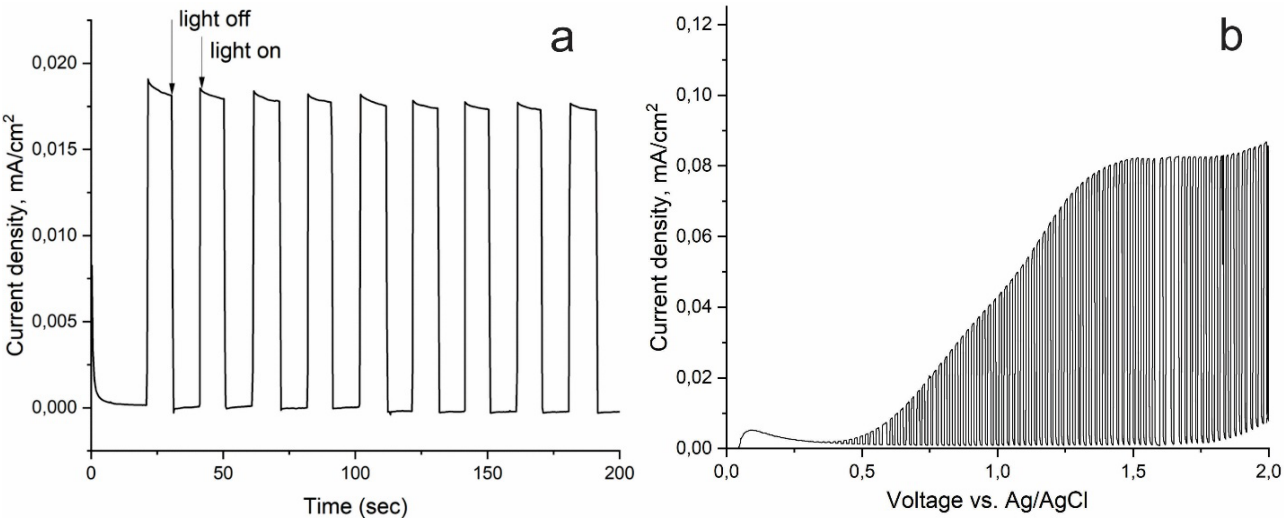

Figure 5 – (a) Photocurrent response of WO_3 electrode at 0.5 V vs. Ag/AgCl and (b) LSV curves in 0.5 M H_2SO_4 aqueous solution under solar irradiation

4 Conclusion

In conclusion, this study demonstrated a successful synthesis of hierarchical WO_3 microspheres through a chemical bath deposition method, highlighting their unique morphology characterized by spontaneous self-assembled nanosheets. The investigation of structural properties using X-ray diffraction and Raman spectroscopy revealed the monoclinic modification of the synthesized particles. In addition, the optical analysis using UV-Vis diffuse reflectance absorption spectra revealed a notable energy gap of 2.2 eV, demonstrating the material's exceptional light absorption capabilities.

The WO_3 photoelectrode exhibited a remarkable photocurrent density of 18 μA/cm^2 at 0.5 V, highlighting the enhanced light absorption and photocatalytic performance attributed to the elongated structures within the microspheres.

These findings indicate the potential of hierarchical WO_3 microspheres as promising candidates for various applications, particularly in the field of photocatalysis, where their high specific surface area and improved light absorption make them a valuable asset for harnessing solar energy and promoting sustainable environmental solutions.

Acknowledgments

This research was funded by Program of the Committee of Science of the Ministry Science Higher Education of the Republic of Kazakhstan, grant number №AP19679991 for 2023-2025. The authors express their gratitude's to Texas Tech University (USA).

References

1. Shabdan Y., et al. Photoactive tungsten-oxide nanomaterials for water-splitting // Nanomaterials. – 2020. – Vol.10. no. 9: 1871. https://doi.org/10.3390/nano10091871

2. Afroz K., et al. A heterojunction strategy to improve the visible light sensitive water splitting performance of photocatalytic materials // Journal of Materials Chemistry A.-2018. – Vol.6. – no.44. – P. 21696-21718. https://doi.org/10.1039/C8TA04165B

3. Bozheyev F., et al. Band gap optimization of tin tungstate thin films for solar water oxidation // International Journal of Hydrogen Energy. – 2020 – Vol.45. – no.15 – P. 8676-8685. http://dx.doi.org/10.1016/j.ijhydene.2020.01.126

4. Markhabayeva A., et al. Effect of synthesis method parameters on the photocatalytic activity of tungsten oxide nanoplates //AIP Advances. – 2021.- Vol. 11. – no. 9 https://doi.org/10.1063/5.0065156

5. Abdullin K.A., et al. Core–shell (W@ WO3) nanostructure to improve electrochemical performance // ACS Applied Energy Materials. – 2018. – Vol. 2. – no.1 – P. 797-803. https://doi.org/10.1021/acsaem.8b01869

6. Markhabayeva A.A., et al. Designing of WO3@Co3O4 heterostructures to enhance photoelectrochemical performances // The Journal of Physical Chemistry A. – 2019. – Vol. 124.3.- P. 486-491. https://doi.org/10.1021/acs.jpca.9b09173

7. Prikhodko O.Y. et al. Photocatalytic activity of liquid-phase exfoliated gallium selenide flakes // Chalcogenide Letters. – 2021. – Vol. 18. – no.12. – P. 777-781. https://doi.org/10.15251/cl.2021.1812.777

8. Marhabaeva A., et al. Preparation method of tungsten oxide and metallic tungsten nano-powders using degreased cotton // Physical Sciences and Technology. – 2018. – Vol. 4. – no.2 – P. 48-53. https://doi.org/10.26577/phst-2017-2-133

9. McPeak, K.M., et al. Chemical bath deposition of ZnO nanowires at near-neutral pH conditions without hexamethylenetetramine (HMTA): understanding the role of HMTA in ZnO nanowire growth // Langmuir. – 2011. – Vol. 27. – no.7. – P. 3672-3677. http://dx.doi.org/10.1021/la105147u

10. Abdullin, K.A., et al. Electrical, optical, and photoluminescence properties of ZnO films subjected to thermal annealing and treatment in hydrogen plasma // Semiconductors. – 2016. – Vol. 50. – P. 1010-1014. http://dx.doi.org/10.1134/S1063782616080029

11. Kaningini, A.G., et al. Effect of Optimized Precursor Concentration, Temperature, and Doping on Optical Properties of ZnO Nanoparticles Synthesized via a Green Route Using Bush Tea (Athrixia phylicoides DC.) Leaf Extracts // ACS omega. – 2022. Vol. 7. – no.36. – P. 31658-31666. https://doi.org/10.1021/acsomega.2c00530

12. Mussabek G.K., Yermukhamed D., Dikhanbayev, K.K., Mathur, S., Sivakov V. Self-organized growth of germanium nanocolumns // Materials Research Express. – 2017. Vol. 4(3). 035003. https://doi.org/10.1088/2053-1591/aa5ed6

13. Wang, D., et al. Synthesis of g-C3N4/NiO p–n heterojunction materials with ball-flower morphology and enhanced photocatalytic performance for the removal of tetracycline and Cr 6+ // Journal of Materials Science. – 2019. Vol. 54. – P. 11417-11434. https://doi.org/10.1007/s10853-019-03692-5

14. Zhang, J., et al. B doped Bi2O2CO3 hierarchical microspheres: Enhanced photocatalytic performance and reaction mechanism for NO removal // Catalysis Today. – 2021. Vol. 380. – P. 230-236. https://doi.org/10.1016/j.cattod.2020.11.009

15. Guo, S.-q., et al. "Facile preparation of hierarchical Nb 2 O 5 microspheres with photocatalytic activities and electrochemical properties. Journal of Materials Chemistry A. – 2014. – Vol. 2. – no.24. – P. 9236-9243. https://doi.org/10.1039/C4TA01567C

16. Parthibavarman, M., et al. Facile and one step synthesis of WO_3 nanorods and nanosheets as an efficient photocatalyst and humidity sensing material // Vacuum. – 2018. – Vol. 155. – P. 224-232. https://doi.org/10.1016/j.vacuum.2018.06.021

17. Wang, M., et al. WO3 porous nanosheet arrays with enhanced low temperature NO2 gas sensing performance // Sensors and Actuators B: Chemical. – 2020. – Vol. 316. – P. 128050. https://doi.org/10.1016/j.snb.2020.128050

18. Bao M., et al. Plate-like p–n heterogeneous NiO/WO3 nanocomposites for high performance room temperature NO2 sensors // Nanoscale. – 2014. – Vol. 6. – no.8. – P. 4063-4066. https://doi.org/10.1039/C3NR05268K

19. Markhabayeva A., et al. Effect of synthesis method parameters on the photocatalytic activity of tungsten oxide nanoplates // AIP Advances. – 2021. – Vol. 11. – no.9. https://doi.org/10.1063/5.0065156

20. Ma J., et al. Topochemical preparation of WO3 nanoplates through precursor H2WO4 and their gas-sensing performances // The Journal of Physical Chemistry C. – 2011. Vol. 115. no.37. – P. 18157-18163. https://doi.org/10.1021/jp205782a

21. Meng, D., et al. Synthesis of WO3 flower-like hierarchical architectures and their sensing properties // Journal of Alloys and Compounds. – 2015. Vol. 649. – P. 731-738. https://doi.org/10.1016/j.jallcom.2015.07.142

22. Lisnyak, V.V., Mussabek, G.K., Zhylkybayeva, N.Zh., Baktygerey, S.Z., Zaderko, A.N. Preparation and Characterization of Carbon-Silicon Hybrid Nanostructures // Journal of Nano- and Electronic Physics. – 2021. – Vol. 13(5). – P. 1-5. https://doi.org/10.21272/jnep.13(5).05035

23. Diyuk, N.V., Keda, T.Y., Zaderko, A.N., .Mussabek, G.K., Kutsevol, N.V., Lisnyak, V.V. Luminescent carbon nanoparticles immobilized in polymer hydrogels for pH sensing // Applied Nanoscience (Switzerland). – 2022. – Vol. 12(8). -P. 2357 – 2365. https://doi.org/10.1007/s13204-022-02536-0

24. Daniel, M., et al. Infrared and Raman study of WO3 tungsten trioxides and WO3, xH2O tungsten trioxide tydrates // Journal of solid state chemistry. – 1987. – Vol. 67. no.2. – P. 235-247. https://doi.org/10.1016/0022-4596(87)90359-8

25. Rougier A., et al. Characterization of pulsed laser deposited WO3 thin films for electrochromic devices // Applied Surface Science. – 1999. – Vol. 153. – no.1. – P. 1-9. https://doi.org/10.1016/S0169-4332(99)00335-9

26. Zhang, S., et al. Controllable syntheses of hierarchical WO3 films consisting of orientation-ordered nanorod bundles and their photocatalytic properties // Crystal Growth & Design. – 2018. Vol. 18. – no.2. – P. 794-801. https://doi.org/10.1021/acs.cgd.7b01254

27. Díaz-Reyes J., et al. Characterization of WO 3 thin films grown on silicon by HFMOD // Advances in Condensed Matter Physics. – 2013. https://doi.org/10.1155/2013/591787

28. González-Borrero P., et al. Optical band-gap determination of nanostructured WO3 film // Applied Physics Letters. – 2010. – Vol. 96. – no.6. https://doi.org/10.1063/1.3313945

29. Yao, Y., et al. A review on the properties and applications of WO3 nanostructure-based optical and electronic devices // Nanomaterials. 2021. – Vol. 11. – no. 8. – P. 2136. https://doi.org/10.3390/nano11082136

30. Johansson M.B., et al. Optical properties of nanocrystalline WO3 and WO3-x thin films prepared by DC magnetron sputtering // Journal of Applied Physics. – 2014. – Vol. 115. – no. 21. https://doi.org/10.1063/1.4880162

31. Kwong W., et al. Photoelectrochemical properties of WO3 thin films prepared by electrodeposition // Energy Procedia. – 2013. – Vol. 34. – P. 617-626. https://doi.org/10.1016/j.egypro.2013.06.793

32. Thakur, A.K., et al. Controlled synthesis of WO3 nanostructures: optical, structural and electrochemical properties // Materials Research Express. 2018. – Vol. 6. – no. 2. – P. 025006. https://doi.org/10.1088/2053-1591/aae991